



HAL
open science

Detection of wildtype Merkel cell polyomavirus genomic sequence and VP1 transcription in a subset of Merkel cell carcinoma

Thibault Kervarrec, Silke Appenzeller, Anne Tallet, Marie-Laure Jullie, Pierre Sohier, Francois Guillonneau, Arno Rütten, Patricia Berthon, Yannick Le Corre, Ewa Hainaut-Wierzbicka, et al.

► To cite this version:

Thibault Kervarrec, Silke Appenzeller, Anne Tallet, Marie-Laure Jullie, Pierre Sohier, et al.. Detection of wildtype Merkel cell polyomavirus genomic sequence and VP1 transcription in a subset of Merkel cell carcinoma. *Histopathology*, 2023, 84 (2), pp.356-368. 10.1111/his.15068 . hal-04325836

HAL Id: hal-04325836

<https://hal.science/hal-04325836>

Submitted on 6 Dec 2023


HAL is a multi-disciplinary open access archive for the deposit and dissemination of scientific research documents, whether they are published or not. The documents may come from teaching and research institutions in France or abroad, or from public or private research centers.

L'archive ouverte pluridisciplinaire **HAL**, est destinée au dépôt et à la diffusion de documents scientifiques de niveau recherche, publiés ou non, émanant des établissements d'enseignement et de recherche français ou étrangers, des laboratoires publics ou privés.



Distributed under a Creative Commons Attribution - NonCommercial - NoDerivatives 4.0 International License

Detection of wildtype Merkel cell polyomavirus genomic sequence and VP1 transcription in a subset of Merkel cell carcinoma

Thibault Kervarrec,^{1,2}  Silke Appenzeller,³ Anne Tallet,⁴ Marie-Laure Jullie,⁵ Pierre Sohier,^{6,7} Francois Guillonnet,⁸ Arno Rütten,⁹ Patricia Berthon,² Yannick Le Corre,¹⁰ Ewa Hainaut-Wierzbicka,¹¹ Astrid Blom,¹² Nathalie Beneton,¹³ Guido Bens,^{14,15} Charline Nardin,¹⁶ Francois Aubin,¹⁶ Monica Dinulescu,^{17,18} Sebastien Visée,¹⁹ Michael Herfs,²⁰ Antoine Touzé,² Serge Guyétant,^{1,2} Mahtab Samimi,^{2,21} Roland Houben²² & David Schrama²²

¹Department of Pathology, Université de Tours, Centre Hospitalier Universitaire de Tours, ²“Biologie des Infections à Polyomavirus” Team, UMR INRAE ISP 1282, Université de Tours, Tours, France, ³Comprehensive Cancer Center Mainfranken, University Hospital of Würzburg, Würzburg, Germany, ⁴Platform of Somatic Tumor Molecular Genetics, Université de Tours, Centre Hospitalier Universitaire de Tours, Tours, ⁵Department of Pathology, Hôpital Haut-Lévêque, CHU de Bordeaux, CARADERM Network, Pessac, ⁶Faculté de Médecine, Université Paris Cité, ⁷Department of Pathology, Hôpital Cochin, AP-HP.Centre-Université Paris Cité, ⁸3P5 Proteomics, Hôpital Cochin, AP-HP, Centre-Université Paris Cité, Paris, France, ⁹Dermatopathology Friedrichshafen, Germany, ¹⁰Dermatology Department, LUNAM Université, CHU Angers, Angers, ¹¹Dermatology Department, Université de Poitiers, CHU de Poitiers, Poitiers, ¹²Department of General and Oncologic Dermatology, CARADERM Network Ambroise-Paré hospital, APHP & Research Unit EA 4340, University of Versailles-Saint-Quentin-en-Yvelines, Paris-Saclay University, Boulogne-Billancourt, ¹³Dermatology Department, CHR Le Mans, Le Mans, ¹⁴Dermatology Department, CHR d'Orléans, Orléans, ¹⁵Dermatology Department, CH de Blois, Blois, ¹⁶Dermatology Department, Inserm 1098, Université de Franche Comté, CHU Besançon, Besançon, ¹⁷Dermatology Department, CHR Rennes, ¹⁸Institut Dermatologique du Grand Ouest (IDGO), Rennes, ¹⁹Department of Pathology, Centre Hospitalier d'Angoulême, Angoulême, France, ²⁰Laboratory of Experimental Pathology, GIGA-Cancer, University of Liège, Liège, Belgium, ²¹Departement of Dermatology, Université de Tours, Centre Hospitalier Universitaire de Tours, Tours, France and ²²Department of Dermatology, Venereology and Allergology, University Hospital Würzburg, Würzburg, Germany

Date of submission 20 July 2023

Accepted for publication 24 September 2023

Kervarrec T, Appenzeller S, Tallet A, Jullie M-L, Sohier P, Guillonnet F, Rütten A, Berthon P, Le Corre Y, Hainaut-Wierzbicka E, Blom A, Beneton N, Bens G, Nardin C, Aubin F, Dinulescu M, Visée S, Herfs M, Touzé A, Guyétant S, Samimi M, Houben R & Schrama D

(2023) *Histopathology*. <https://doi.org/10.1111/his.15068>

Detection of wildtype Merkel cell polyomavirus genomic sequence and VP1 transcription in a subset of Merkel cell carcinoma

Aims: Merkel cell carcinoma (MCC) is frequently caused by the Merkel cell polyomavirus (MCPyV). Characteristic for these virus-positive (VP) MCC is MCPyV integration into the host genome and truncation of the viral oncogene Large T antigen (LT), with

full-length LT expression considered as incompatible with MCC growth. Genetic analysis of a VP-MCC/trichoblastoma combined tumour demonstrated that virus-driven MCC can arise from an epithelial cell. Here we describe two further cases of VP-MCC

Address for correspondence: T Kervarrec, Department of Pathology, Hôpital Trousseau, CHRU de Tours, 37044 TOURS Cedex 09, France.
e-mail: thibaultkervarrec@yahoo.fr

© 2023 The Authors. *Histopathology* published by John Wiley & Sons Ltd.

This is an open access article under the terms of the [Creative Commons Attribution-NonCommercial-NoDerivs](https://creativecommons.org/licenses/by-nc-nd/4.0/) License, which permits use and distribution in any medium, provided the original work is properly cited, the use is non-commercial and no modifications or adaptations are made.

combined with an adnexal tumour, i.e. one trichoblastoma and one poroma.

Methods and results: Whole-genome sequencing of MCC/trichoblastoma again provided evidence of a trichoblastoma-derived MCC. Although an MCC-typical LT-truncating mutation was detected, we could not determine an integration site and we additionally detected a wildtype sequence encoding full-length LT. Similarly, Sanger sequencing of the

Keywords: Merkel cell carcinoma, polyomavirus, replication, trichoblastoma, VP1

Introduction

Merkel cell carcinoma (MCC) is a rare aggressive skin cancer with a 5-year overall survival estimated at 40%.¹ In 2008, Feng *et al.* discovered a polyomavirus integrated into the genome of MCC cancer cells.² Indeed, association of MCC with Merkel cell polyomavirus (MCPyV) is observed in about 80% of cases, and the virus-encoded two T antigens, i.e. small t (st) and Large T (LT), are considered the crucial drivers of oncogenesis of VP-MCC.³ Importantly, the viral LT has so far always been found to be encoded as a truncated protein (trLT) in MCC, due to stop codon mutations or integration-related deletions in the viral sequence. This suggests that the C-terminus of LT containing a helicase and an origin binding-domain necessary for MCPyV genome replication and expression of the capsids proteins,^{2,4,5} might be incompatible with tumour development.⁴ Indeed, the growth inhibitory properties of the C-terminus of LT have been demonstrated.⁶ Besides trLT, the only other viral protein found to be regularly expressed in MCC tumour cells is small T, whereas the structural capsid proteins, i.e. VP1 and VP2, appear not to be expressed.^{2,4,5} Moreover, replication of the viral genome could not be detected in VP-MCC.^{2,4,5} In contrast, MCPyV replication might occur in dermal fibroblasts, which have been suggested as the primary target cells of MCPyV in the skin.⁷ However, the cell in which MCC originates was for a long time a matter of debate, with either epithelial progenitors or non-epithelial cells being discussed as candidates.^{1,7–11}

Combined tumours associating an MCC tumour with another differentiation subset account for 5 to 10% of all MCC cases.¹² Most of these cases are composed of a malignant squamous cell carcinoma component and an MCPyV-negative MCC.^{13–15} However, we recently demonstrated expression of the MCPyV LT in two exceptional tumour specimens comprising a

combined MCC/poroma revealed coding sequences for both truncated and full-length LT. Moreover, *in situ* RNA hybridization demonstrated expression of a late region mRNA encoding the viral capsid protein VP1 in both combined as well as in a few cases of pure MCC.

Conclusion: The data presented here suggest the presence of wildtype MCPyV genomes and VP1 transcription in a subset of MCC.

trichoblastoma and an MCC part.¹⁶ Moreover, massive parallel sequencing of one case demonstrated that MCPyV integration in a trichoblastoma cell gave rise to the VP-MCC component,¹⁶ demonstrating that VP-MCC can have an epithelial origin. Importantly, in addition to the integrated MCPyV encoding trLT in the MCC part, wildtype MCPyV genome as well as LT expression was detected in the trichoblastoma part of the combined tumour. This not only suggests that MCPyV replication might have occurred in these epithelial follicular cells, but also that the presence of a wildtype MCPyV expressing full-length LT is tolerated under certain circumstances by tumour cells.

To further exploit the combined VP-MCC as a model for MCPyV-induced MCC oncogenesis, we here present analysis of two further combined tumours comprising MCC and an adnexal component and compare these cases with a large cohort of pure MCC. Surprisingly, we provide evidence for wildtype MCPyV genome replication and VP1 mRNA expression in some combined and pure MCC cases.

Methods

PATIENTS AND SAMPLES

Combined Case #1 was identified from our consultation cases, cases #2 was extracted from the literature. Other MCC cases (local ethics committee, Tours, France; no. ID RCB2009-A01056-51) were selected from an historical/prospective cohort of MCC patients from six French hospital centers, as described previously with only MCPyV-positive cases included in the present analysis.¹⁷

CLINICAL AND FOLLOW-UP DATA

Age, sex, immunosuppression (HIV infection, organ transplant recipient, haematological malignancies),

American Joint Committee on Cancer (AJCC) stage at the time of surgery,¹⁸ location of the primary tumour, and follow-up were collected from patient files.

IMMUNOHISTOCHEMISTRY

Immunohistochemical staining for Cytokeratin 20, Large T Antigen (AB3 and CM2B4), and SATB2 was performed using a BenchMark XT Platform as instructed.^{17,19} Antibodies and dilutions are provided in the Supplementary Materials.

IN SITU RNA HYBRIDIZATION ANALYSIS

Detection of VP1 RNA was performed using the RNAscope 2.5 HD Reagent Kit-BROWN with the RNAscope Probe VP1 (ACD, Bio-Techne SAS, France) according to the manufacturer's instructions. Briefly, after a drying step for 1 h at 60°C, tissue sections were deparaffinized and pretreated with RNAscope Hydrogen Peroxide for 10 min at room temperature (RT). Antigen retrieval was carried out by boiling the slides at 100°C for 15 min in the RNAscope Target Retrieval Reagents. Then slides were dried before the proteolytic treatment with the RNAscope Protease Plus for 30 min at 40°C in the ACD HyBEZ II Hybridization System. All washes were performed in distilled water. The hybridization signal was revealed with the chromogen diaminobenzidine (DAB). Slides were counterstained with haematoxylin, dehydrated, and mounted with Eukitt.

DNA ISOLATION AND MCPYV QUANTITATIVE POLYMERASE CHAIN REACTION (QPCR)

After microdissection of the two tumour components and of the healthy tissue under a binocular magnifier, genomic DNA was isolated with the use of the Maxwell 16 Instrument (Promega, Madison, WI, USA) with the Maxwell 16 formalin-fixed and paraffin-embedded Plus LEV DNA purification kit (Promega). Of note, dissection of the trichoblastoma was performed in areas devoid of LT expression. MCPyV-LT real-time PCR was performed as described using albumin as reference gene for normalization and the $2^{-\Delta Cq}$ method for quantification.¹⁷ Sequences of the primers used for qPCR are available in the Supplementary Materials.

PCR AMPLIFICATION AND SANGER SEQUENCING

Nested PCRs with primers listed in the Supplementary Materials were performed to amplify the respective regions. PCR reactions were carried out in a total

volume of 20 µl containing 1 × HF buffer, 1 µM of each primer, 200 µM dNTPs, 1 unit Q5 Phusion (NEB), and 1 µl of template. After an initial denaturation at 98°C for 1 min, the thermal profile consisted of denaturation at 98°C for 10 sec, annealing at the optimal temperature for 30 sec, and elongation at 72°C for 1 min (30 cycles for preamplification and 40 cycles for amplification). After PCR purification the amplicons were sent to SeqLab (Microsynth, Balgach, Switzerland) for sequencing.

NEXT-GENERATION SEQUENCING

For the library preparation of the exomes (both tumours and their paired healthy tissue sample) the SureSelectXT Library Prep Kit (Agilent, Palo Alto, CA, USA) was used. Enrichment was performed using Agilent's SureSelectXT Human All Exon V6 Kit. The genomic library (MCC only) was prepared using TruSeq Nano DNA (Illumina, San Diego, CA). Paired end sequencing with a read length of 150 bps was performed on a NovaSeq 6000 (Illumina).

DATA ANALYSIS

An initial quality assessment was performed using FastQC, v0.11.3²⁰ (Andrews S., 2010. Available online at: <http://www.bioinformatics.babraham.ac.uk/projects/fastqc>). Low-quality reads were trimmed with TrimGalore, v0.6.1 (Krueger, F., 2012: Available online at: http://www.bioinformatics.babraham.ac.uk/projects/trim_galore/) powered by Cutadapt, Illumina, v2.3.²¹ The trimmed reads were mapped to the human reference genome (hg19) using BWA mem, v0.7.17²² and sorted and indexed using Picard, v1.125 (available online at: <http://broadinstitute.github.io/picard/>) and SAMtools, v1.3,²³ respectively. Duplicates were marked with Picard. For the exomes, local realignment around indels was executed with GATK, v4.0.11.0.²⁴ GATK, v3.5 was used for coverage calculations.

SOMATIC VARIANT CALLING

MuTect1, v 1.1.4²⁵ was used to identify somatic single nucleotide variants (SNVs) as well as small somatic insertions and deletions (indels). All variants were annotated with ANNOVAR, v2019-10-24.²⁶ Eight somatic variants shared by the trichoblastoma and the MCC were visually examined using the Integrative Genomics Viewer, v2.3.68,²⁷ and confirmed with Sanger sequencing if they have an impact on the protein sequence or affect a splice site, are rare in the population (below a frequency of 2% in 1000g2015aug_all, ExAC_nontcga_ALL, gnomAD_exome_ALL and gnomAD_genome_ALL), and the

position is covered by at least 20 reads and the alternative allele is covered by at least eight reads and frequency is at least 5%. Mutational signatures were identified using COSMIC Mutational Signatures v2²⁸ investigating somatic variants with at least 10% frequency.

DETECTION OF THE VIRUS INTEGRATION SITE

Seeksv, v1.2.3²⁹ was used with the human reference genome sequence (hg19) and the MCPyV MCC350 genome sequence (GenBank EU375803) to detect the virus integration site.

Results

POSSIBLE MCPYV-INDUCED ONCOGENESIS OF COMBINED MCCS HARBOURING A BENIGN ADNEXAL COMPONENT

MCC associated with a trichoblastoma is a very rarely observed tumour combination. Nevertheless, in addition to the recently published two combined trichoblastoma/MCC¹⁶ we could identify a further case of a combined tumour harbouring benign trichoblastoma and MCC components (Case #1). Clinical and microscopic features of the case are given in Figure 1, Table S1. Briefly, the specimen consisted of a 4-mm diameter nodule located on the eyelid. Microscopic examination revealed a well-delimited tumour located in the dermis and consisting of two distinct components, i.e. trichoblastoma and MCC, with some transition areas containing tumour cells with MCC-like cytological features included in the trichoblastoma component (Figure 1). Real-time PCR revealed the presence of MCPyV, suggesting a virus-induced carcinogenesis of the MCC, and detection of MCPyV LT expression in the MCC cells by immunohistochemistry supported this view. Importantly, however, LT expression was also observed in the trichoblastoma part and was not restricted to the cells expressing Merkel cell markers, but was additionally detected in pure trichoblastoma areas (Figure 1). This was associated with a very high viral load of 240 copies/cell determined in DNA derived from the complete specimen.

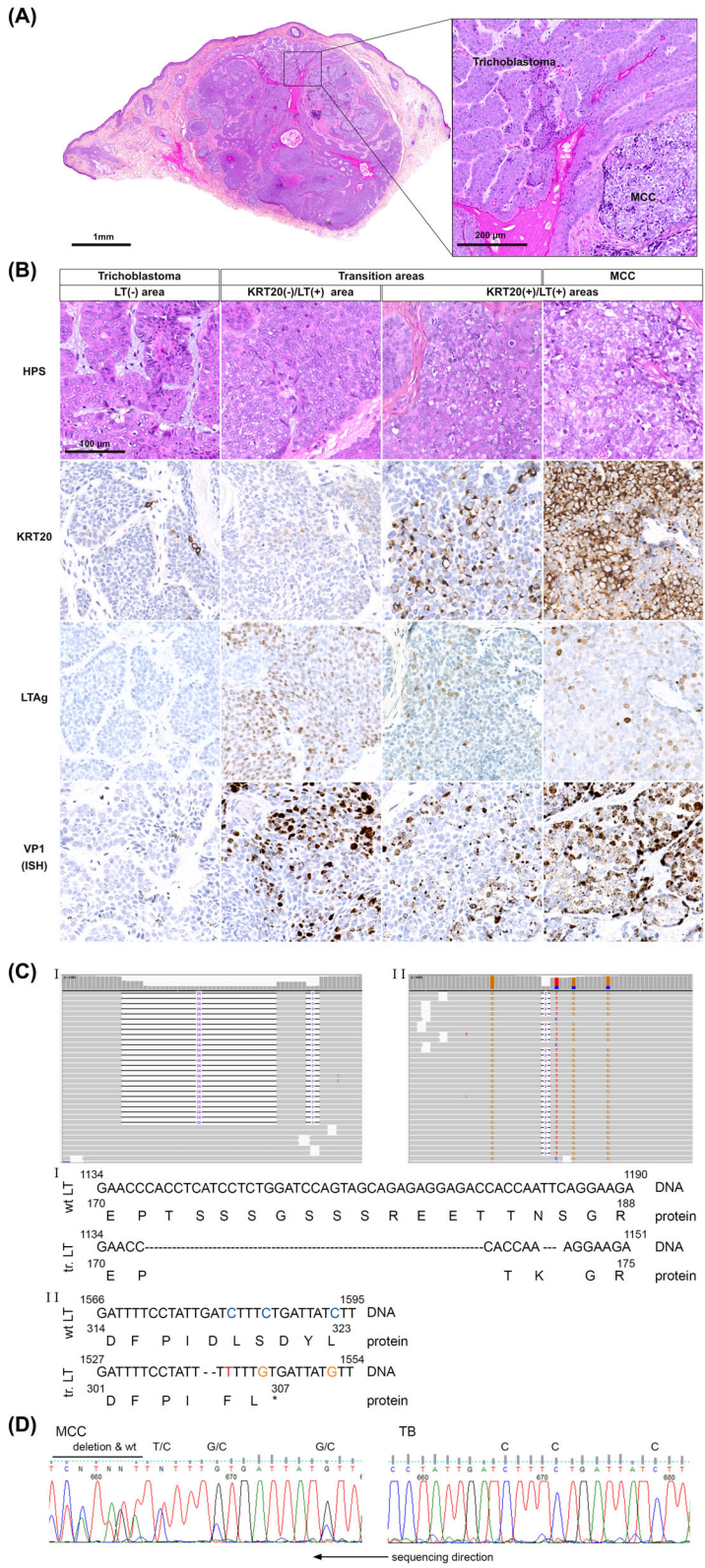
After having confirmed the MCPyV presence in a total of three combined trichoblastoma/MCC, we asked whether other combined MCC harbouring a benign adnexal component might—in contrast to the prototypic combined SCC/MCC—be characterized by presence of MCPyV. By carefully reviewing the literature (Table S1) we could identify 10 additional cases describing MCC combined with trichilemmal ($n = 4$), follicular cysts ($n = 3$), or with poroma ($n = 3$).^{30–35} Among them, one MCC/poroma case (Case #2) (Figure 2) was available for further immunohistochemical and molecular characterization.³² Poromas are rare benign tumours originating from the intraepidermal portion of the sweat gland duct.³⁶ Immunohistochemistry of the combined MCC/poroma revealed expression of MCPyV-LT in both components, with staining intensities varying from strong/moderate in the MCC to weak/inconspicuous in the poroma part (Figure 2). Real-time PCR, performed with DNA derived from the complete specimen, confirmed again a relatively high (mean) viral load of 80 MCPyV copies/cell.

Together with the two previously published cases,¹⁶ these data demonstrate involvement of MCPyV in four out of four analysed combined tumours comprising an MCC and an adnexal component.

COEXISTENCE OF WILDTYPE AND MUTATED MCPYV ENCODING FULL-LENGTH AND TRUNCATED LT, RESPECTIVELY

To further characterize such combined tumours, pure areas of trichoblastoma and MCC from Case #1 were microdissected, allowing DNA extraction and massive parallel sequencing using healthy tissue (peripheral blood mononuclear cells) as reference (Tables S2 and S3). In line with a potential virus-induced oncogenesis in this case, our analysis revealed low tumour mutational burden and a lack of UV signature in the MCC component, but also in the trichoblastoma. Importantly, all eight somatic variants detected in the trichoblastoma part were shared by the MCC, implying a shared clonal origin of the two tumour components (Table S3). Both components were distinguishable by only the MCC harbouring MCPyV

Figure 1. Microscopic and molecular features of the trichoblastoma/VP-MCC combined tumour. (A) Combined tumour consisting of a MCC and trichoblastoma component. (B) Transition areas between the two tumour components were present and highly mitotic tumour cells were found in the MCC part. In some areas, trichoblastic cells expressed LT without evidence of MCC transformation, while in another part small clusters of tumour cells with MCC morphology and KRT20 expression were entrapped into the trichoblastoma. RNAscope analysis demonstrated VP1 expression throughout all parts. (C) Whole-genome sequencing identified two distinct MCPyV sequences distinguishable by deletions and single nucleotide polymorphisms. (D) Sanger sequencing revealed the coexistence of wildtype and mutated MCPyV genome in the MCC component and only a WT sequence in the trichoblastoma.



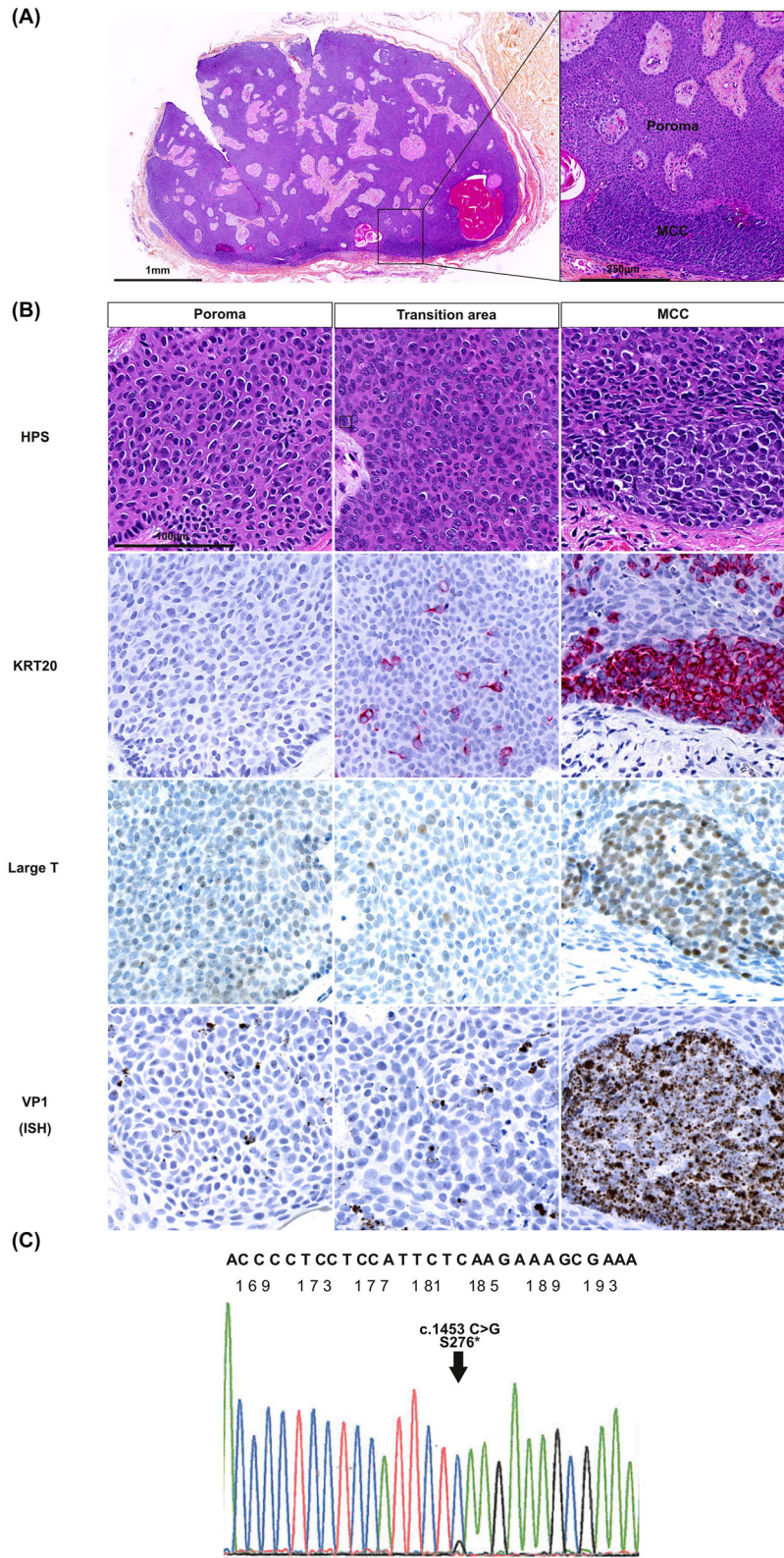


Figure 2. Microscopic and molecular features of the poroma/VP-MCC combined tumour. (A) Microscopic inspection revealed a tumour consisting of dermal and subcutaneous well-delimited tumour nodules with massive and “Pinkus-like” growth pattern. (B) The tumour was mostly composed of small nonatypical poroid cells associated in the periphery with small clusters of MCC tumour cells expressing KRT20 and MCPyV LT. LT protein and VP1 mRNA expression were observed in both the trichoblastoma and MCC part with high intensity only in the latter. (C) PCR amplification of LT encoding MCPyV sequences followed by Sanger sequencing revealed the coexistence of a wildtype and a mutated genome in this specimen.

sequences encoding a trLT of 306 amino acids (stop codon created by frameshift causing deletion). Although this hallmark of VP-MCC was present,⁴ in addition to the mutated MCPyV genome, wildtype sequences were not only detectable but even predominant (around 76% of the reads) in the MCC. Interestingly, the mutant viral DNA was probably not a derivative of the copresent wildtype virus since, in addition to the truncating mutation, the two viral sequences differed with respect to several single nucleotide polymorphisms (SNPs) and two short in-frame deletions (Figure 1). In the trichoblastoma-derived DNA we detected only wildtype MCPyV. Neither in the trichoblastoma, but surprisingly also not in the MCC DNA, we were able to detect insertion of viral sequences in the host cell genome by our sequencing approach.

Unfortunately, for the second combined MCC (Case #2) we did not have sufficient tumour material allowing whole-exome or genome sequencing. Therefore, PCR amplification of MCPyV sequences followed by Sanger sequencing was performed on the whole specimen, leading to the identification of an MCC-characteristic stop codon mutation in LT following the Rb binding motif, confirming this hallmark of MCPyV-induced MCC development. Importantly, however, again the mutated MCPyV sequence (S276*) yielded only a background signal within a predominant MCPyV wildtype sequence (Figure 2).

In summary, on the one hand, the presence of the virus and characteristic LT-truncating mutations suggest frequent MCPyV-induced oncogenesis of combined MCCs harbouring an additional benign adnexal component. On the other hand, however, the coexistence of replicative competent wildtype and replicative deficient mutated MCPyV in the MCC cells is unexpected, and might be a characteristic feature of this subgroup.

EVIDENCE OF MCPyV REPLICATION IN A SUBSET OF COMBINED AND PURE MCC

To evaluate whether the observed presence of wildtype MCC represents a specific feature of MCC combined with adnexal tumours, we compared those

with pure MCCs. The presence of wildtype MCPyV might imply ongoing viral replication in the tumour cells, i.e. genome replication leading to high viral load and expression of capsid proteins. To test this, we first compared MCPyV viral loads determined by real-time PCR in the combined tumours and in a previously described large cohort of VP-MCC ($n = 174$) (median MCPyV load of the whole cohort = 10 copies/cell, Q1-Q3: 6–17) (Figure 3). Interestingly, the two combined cases described here¹⁶ were among the MCCs with the highest viral loads (Ranks: 6, and 7/177, respectively). Together with five pure MCCs they constituted, with respect to viral load, a clearly distinct subgroup (MCPyV load >70, Median: 358 copies/cell, Q1-Q3: 247–7861) compared to the remaining MCCs (Median MCPyV load: 9, Q1-Q3: 6–17). Characteristics of these five high viral load pure MCC cases are available in Table S4.

Next we tested whether wildtype MCPyV might also contribute to the high viral load in pure MCCs. To this end, PCR amplification of MCPyV and Sanger sequencing was performed in the five cases with the highest MCPyV load. Indeed, this analysis demonstrated the presence of both mutant and wildtype MCPyV sequences encoding full-length LT in two cases (Figure 3, Table S4) and in one other MCC, which had the highest MCPyV load, even only the wildtype sequence was detectable. In one case we detected only mutant MCPyV sequences, while for the fifth case we did not get interpretable sequencing results due to poor DNA quality.

Since expression of wildtype LT can be expected to result in VP1 expression,⁴ we assessed VP1 gene transcription using *in situ* RNA hybridization on tissue sections of the two combined cases (Cases #1 and #2; Figures 1 and 2) and in the complete MCC cohort included in a tissue microarray (Figure 3). Such analysis revealed in both combined tumours expression of VP1 in the two components with higher levels observed in the MCC part. Moreover, in the complete MCC cohort, diffuse, intense signal present in all tumour cells was detected in 10 cases (Table S4), including five of the previously identified MCCs harbouring a very high viral load. Interestingly, in one case, analysis of primary tumour and metastasis

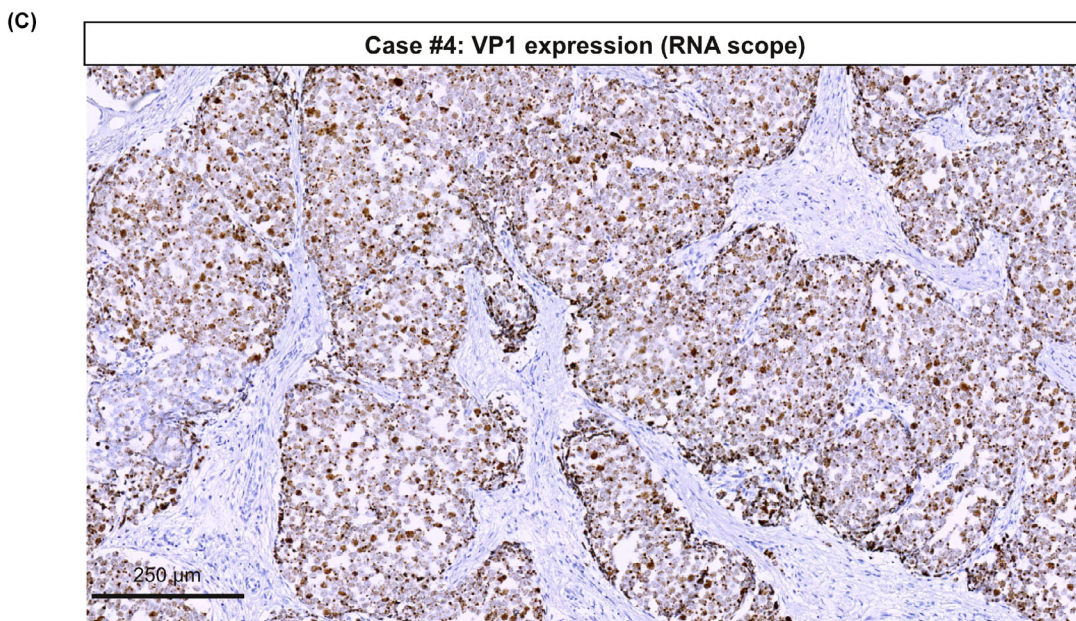
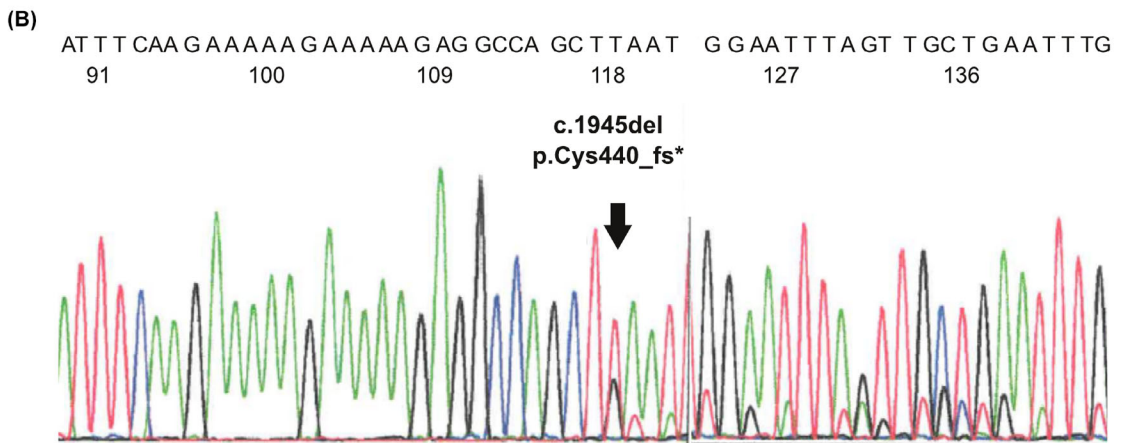
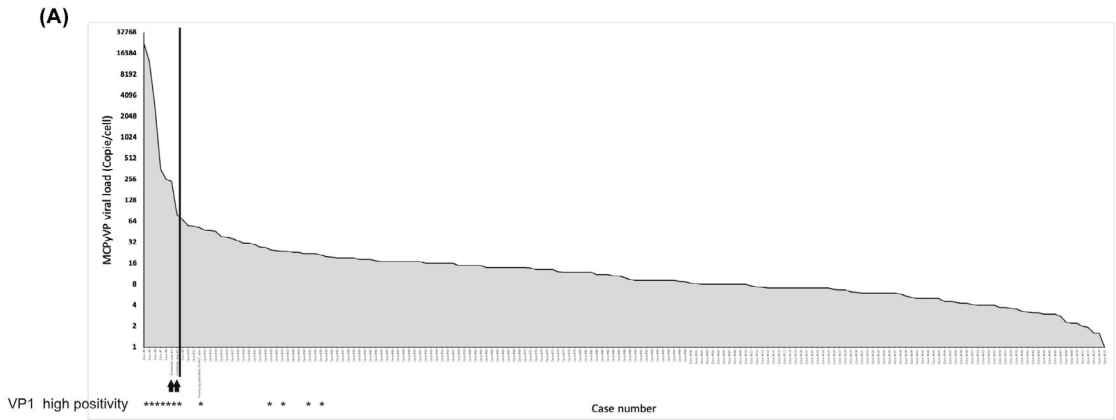


Figure 3. Detection of wildtype genome and VP1 transcription in a subset of pure MCC tumours. (A) Real-time PCR to determine MCPyV viral loads in DNA derived from a large cohort ($n = 177$) of pure VP-MCC cases and the two combined tumours described here. Results (genome copy number/cells) are depicted from high to low viral loads. Black stars indicate the cases in which intense VP1 expression was detected by RNAscope. (B) PCR amplification of LT encoding MCPyV sequences followed by Sanger sequencing revealed the coexistence of a wildtype and a mutated genome in Case #6 (MCPyV load = 358 copies/cell). (C) Representative illustration of VP1 transcript *in situ* detection by RNAscope (MCC Case #6).

revealed the same features, i.e. high MCPyV viral load and diffuse VP1 expression in both specimens.

MCPyV INFECTION OF HUMAN HAIR FOLLICLE CELLS

In line with recently published mouse models demonstrating TA-induced MCC-like tumour formation in the hair follicle,^{11,37} derivation of VP-MCC from trichoblastoma cells suggests that hair follicle cells might contain the cells of origin for MCPyV-induced carcinogenesis. A prerequisite for such a scenario would be the capability of MCPyV to infect the hair follicle. Indeed, among the 10 pure MCC cases expressing VP1 transcripts, we identified an MCC case consisting of a small dermal 1.2-mm diameter tumour located on the cheek. Microscopic examination of this specimen revealed in addition to the dermal invasive part, an *in situ* MCC component located in the inner root sheath of the hair follicle (Figure 4). Immunohistochemistry using two different antibodies revealed expression of MCPyV LT in cells of the inner root sheath. As suggested by their morphology and the absence of MCC markers, these LT-positive hair follicle cells were not tumour cells. Sanger sequencing of LT in DNA derived from a complete tumour section (microdissection was not feasible) identified both wildtype and truncated LT encoding MCPyV (Figure 4). Wide expression of VP1 was further demonstrated in both hair follicle and MCC tumour cells by *in situ* hybridization. These results are in line with an ongoing MCPyV infection by a wildtype MCPyV in cells of the inner root sheath of the patient's hair follicle. Hence, cells from the epithelial lineage might be a site of MCPyV infection and replication.

Discussion

Although identification of recurrent genomic MCPyV integration in MCC has been a main achievement in our understanding of MCC biology,² the early steps leading to MCC development are still elusive. In this context, the nature of the cells in which MCPyV infection, replication, and integration occur is still a matter of debate.^{1,9,10,38,39} Moreover, it has yet to be

clarified how in MCC development the co-occurrence of LT truncation and MCPyV integration is achieved.⁴ In the present study, analyses of two combined tumours composed of a benign adnexal and an MCC component confirmed the conclusion of previous reports^{11,16,37} that skin epithelial cells can give rise to VP-MCC. Furthermore, we demonstrate the coexistence of MCPyV-genomes encoding either wildtype or truncated LT in the combined tumours, as well as in a small portion of pure MCC cases. Together with the observed high MCPyV viral load as well as the detection of VP1, these findings suggest ongoing MCPyV replication in these tumours.

A quite diverse set of potential MCC ancestors such as neuronal cells, epithelial progenitors, fibroblasts, and pre/pro B cells in which MCPyV integration can give rise to an MCC has been proposed.^{1,9,10,39} Recently, we characterized a rare skin tumour combining an VP-MCC and a trichoblastoma, i.e. a benign tumour exhibiting hair follicle differentiation.¹⁶ Massive parallel sequencing of the two components demonstrated common genetic alterations in both parts of the tumour while MCPyV integration was only observed in the MCC region. Thus, this case demonstrated that MCPyV integration in a trichoblastoma cell, i.e. a follicular epithelial cell, gave rise to a VP-MCC. Further support for this finding comes from two recently published mouse models. Weber *et al.* observed induction of neuroendocrine and Merkel cell markers upon combined sT expression and Rb inactivation (functionally mimicking LT expression) in hair follicle cells,³⁷ while Verhaegen *et al.* demonstrated development of MCC precursor lesions only in the hair follicle upon combined MCPyV T Antigen and *Atoh1* expression in epidermal cells.¹¹

In the present study, we investigated two human combined tumours harbouring an VP-MCC and a benign adnexal component characterized by the coexistence of MCPyV coding for truncated as well as wildtype LT, resulting in high MCPyV viral load and VP1 expression.

Two independent genetic events, i.e. genomic integration and mutation/deletion of the MCPyV genome resulting in an encoded trLT, are virtually constantly observed in MCC tumours.³ While mutation of an

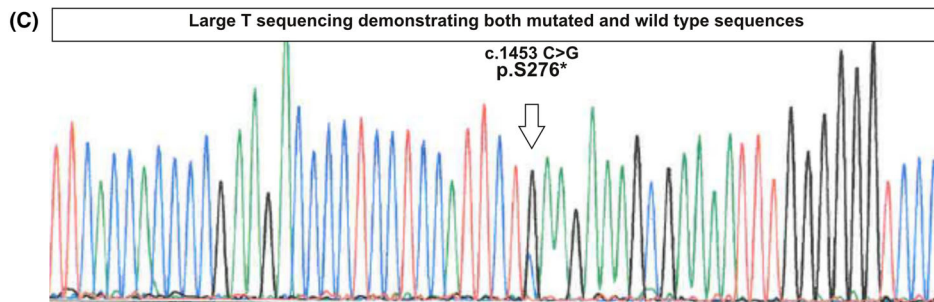
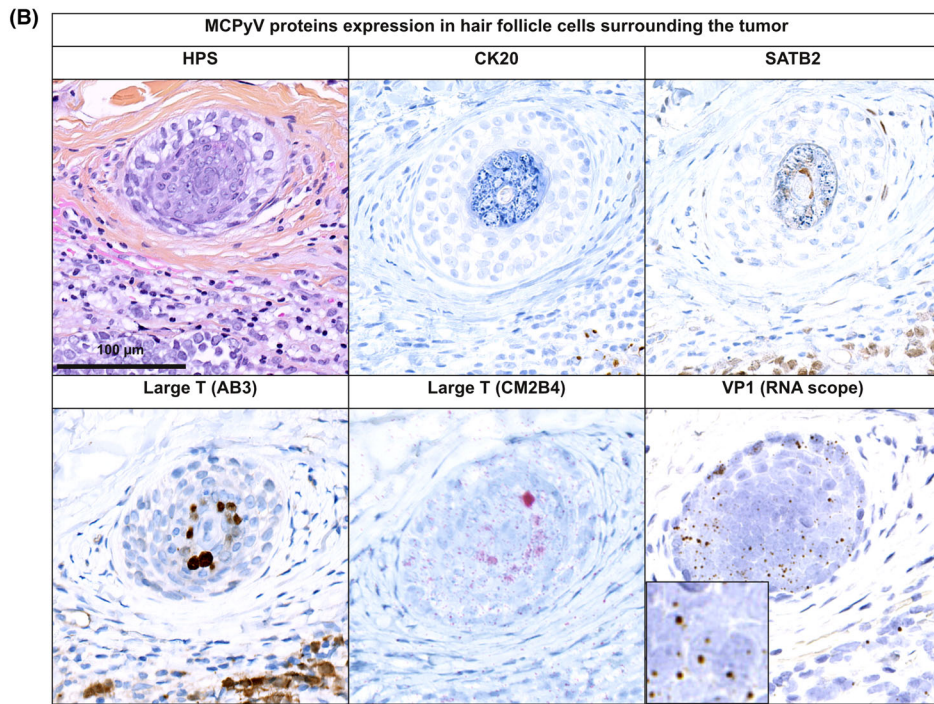
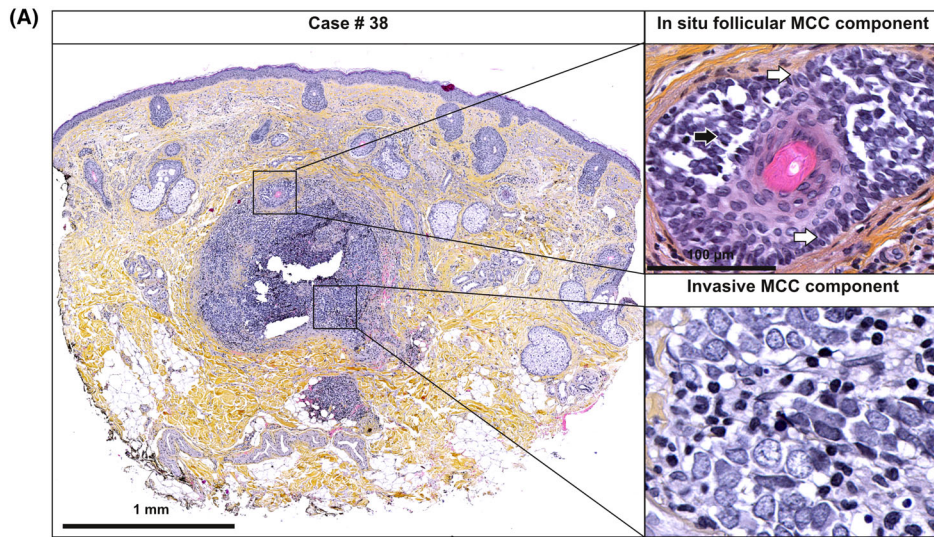


Figure 4. Morphologic and molecular features of a pure VP-MCC tumour with invasive and *in situ* follicular components. (A) The specimen consists of a predominant invasive part of small nodular tumour formation located in the dermis and an associated *in situ* MCC component within a hair follicle. (B) Immunohistochemical investigation, using two different antibodies (Ab3 and CM2B4), revealed LT expression in both, the invasive and the *in situ* tumour part. Moreover, LT was detectable in the hair follicle surrounding the *in situ* tumour, although no expression of the MCC markers KRT20, SATB2 was detected. VP1 mRNA was detected by RNAscope in tumour and hair follicle cells. (C) Sanger sequencing revealed the coexistence of a wildtype and mutated MCPyV in this specimen.

episomal MCPyV genome leading to the expression of a trLT would result in the loss of replicative abilities, resulting in virus strand elimination, integration of a wildtype MCPyV genome and subsequent expression of the full-length LT obviously does not lead to MCC tumour formation.⁴⁰ As potential reasons for incompatibility of full-length LT with tumour formation, growth-inhibitory activities of the LT C-terminus⁶ as well as induction of replication fork collisions by the combination of full-length LT with integrated MCPyV⁴ have been suggested. However, expression of full-length LT in an MCC cell line led to induction of VP1 expression without observing DNA damage or increased cell death in this model.⁴ Similarly, our observations suggest that expression of full-length LT in association with truncated LT can be tolerated by MCC cells, although trLT always being encoded in the tumours indicate their essential role for tumour formation.

Whether LT-truncating mutations occur in the MCPyV genome before or after integration has been a matter to debate.⁴ However, the same stop codons in several concatemerically integrated MCPyV copies suggest that mutations occurred either before or during MCPyV integration.⁴¹ Interestingly, while we detected a premature stop codon in the LT sequence in Case #1, no integration site could be identified. Although this may be due to technical reasons, like the large amount of wildtype sequences and/or insufficient sequencing depth, an alternative explanation is that full-length LT expression allows propagation of episomal wildtype and a mutated MCPyV genome, therefore making virus integration unnecessary. Interestingly, a similar MCC case in which automatic analysis of the sequencing data did not yield an integration site has recently been reported (reference of the case MCC0037).⁴² Manual screening of the sequencing data of this MCC, which is also characterized by a very high viral load, led the authors to propose that the MCPyV genome might be integrated into a retrotransposon element.⁴² A similar integration event might also explain our case. However, the observed VP1 expression, the high viral loads, and coexistence of wildtype and mutated MCPyV are in favour of some episomally replicating virus. Indeed, evidence for ongoing MCPyV replication in some

MCC cases has already been reported. Applying DIPS-PCR to a series of 10 MCC cases, Sastre-Garrau *et al.* identified one MCC with high viral load (62.2 copies per cells) containing wildtype episomal MCPyV coexisting with an integrated mutated form of the virus.⁴³ Furthermore, Haug *et al.* reported a subpopulation of MCC ($n = 7/62$) characterized by high MCPyV viral load and a diffuse detection pattern of MCPyV genomes by fluorescence *in situ* hybridization (FISH).⁴⁴ Therefore, in combination with these previous studies, our results suggest that replication of episomal MCPyV is present in some MCC cases.

Transformation of a trichoblastoma/poroma to an MCC following MCPyV infection suggests that the T antigens are capable of inducing Merkel cell-like features. In this context it is worth noting that two of the key transcription factors involved in Merkel cell differentiation, i.e. ATOH1 and SOX2, are both induced and/or stabilized by MCPyV LT.^{38,45,46} Accordingly, ectopic expression of the T antigens in keratinocytes and hair follicle cells *in vitro* led to the induction of Merkel cell markers like cytokeratin 8, 20, or SATB2.^{46,47} Notably, SATB2 positivity was also detected in T-antigen-expressing hair follicle cells.^{46,47} Accordingly, in one case of the present study, we detected, in a hair follicle close to the tumour, LT and VP1 expression together with SATB2 positivity, while other MCC markers, however, were not detected.

MCPyV-induced transformation of skin appendage-derived cells or even directly of cells from the hair follicle or other appendages suggests that MCPyV is able to infect these cells. Interestingly, expression of MCPyV T antigens in hair follicles has been reported in a case of alopecia.⁴⁸ In addition, we also describe LT/VP1 expression in hair follicle cells in the current study. The respective small-sized (1.2 mm diameter) MCC sample may represent a “young” tumour, which, due to its visible location on the face, was excised early enough to still display initial steps of MCC development allowing detection of a follicular “*in situ*” MCC component as well as adjacent MCPyV-infected hair follicle cells.

To conclude, the current study provides further support for an epithelial origin of MCC by demonstrating that VP-MCC can arise from adnexal tumours. Moreover, evidence of MCPyV replication in

appendages, adnexal, and MCC tumour cells suggests the epithelial lineage as a site of replicative MCPyV infection.

Conflict of interest

The authors declare no conflicts of interest.

Funding information

Interdisziplinäres Zentrum für Klinische Forschung Würzburg (IZKF B-343), German Research Foundation (SCHR 1178/3-1) and Ligue Nationale Contre le Cancer, Comités 16, 18, 28, HUGO Grant.

Author contributions

Thibault Kervarrec, Silke Appenzeller, Roland Houben, and David Schrama equally contributed to the conceptualization, data curation, and formal analysis, Writing - Original Draft Preparation. Mahtab Samimi, Serge Guyétant, and Antoine Touzé contributed to conceptualization, methodology, resources, and validation. Anne Tallet, Marie-Laure Jullie, Pierre Sohier, Francois Guillonneau, Arno Rütten, Patricia Berthon, Yannick Le Corre, Ewa Hainaut-Wierzbicka, Astrid Blom, Nathalie Beneton, Guido Bens, Charline Nardin, Francois Aubin, Monica Dinulescu, Sebastien Visée, and Michael Herfs contributed to investigation, formal analysis, and resources. All authors reviewed, commented, and revised the article.

Institutional review board

The local Ethics Committee of Tours (France) approved the study (no. RCB2009-A01056-51).

Data availability statement

The datasets generated during and/or analysed during the current study will be available in the European Genome-phenome Archive.

References

- Harms PW, Harms KL, Moore PS *et al.* The biology and treatment of Merkel cell carcinoma: current understanding and research priorities. *Nat. Rev. Clin. Oncol.* 2018; **15**: 763–776.
- Feng H, Shuda M, Chang Y, Moore PS. Clonal integration of a polyomavirus in human Merkel cell carcinoma. *Science* 2008; **319**: 1096–1100.
- Houben R, Celikdemir B, Kervarrec T, Schrama D. Merkel cell polyomavirus: infection, genome, transcripts and its role in development of Merkel cell carcinoma. *Cancer* 2023; **15**: 444.
- Shuda M, Feng H, Kwun HJ *et al.* T antigen mutations are a human tumor-specific signature for Merkel cell polyomavirus. *Proc. Natl. Acad. Sci. U.S.A.* 2008; **105**: 16272–16277.
- Touzé A, Le Bidre E, Laude H *et al.* High levels of antibodies against merkel cell polyomavirus identify a subset of patients with merkel cell carcinoma with better clinical outcome. *J. Clin. Oncol.* 2011; **29**: 1612–1619.
- Cheng J, Rozenblatt-Rosen O, Paulson KG, Nghiem P, DeCaprio JA. Merkel cell polyomavirus large T antigen has growth-promoting and inhibitory activities. *J. Virol.* 2013; **87**: 6118–6126.
- Liu W, Yang R, Payne AS *et al.* Identifying the target cells and mechanisms of Merkel cell polyomavirus infection. *Cell Host Microbe* 2016; **19**: 775–787.
- Becker JC, Zur HA. Cells of origin in skin cancer. *J. Invest. Dermatol.* 2014; **134**: 2491–2493.
- Kervarrec T, Samimi M, Guyétant S *et al.* Histogenesis of Merkel cell carcinoma: a comprehensive review. *Front. Oncol.* 2019b; **9**: 451.
- Sunshine JC, Jahchan NS, Sage J, Choi J. Are there multiple cells of origin of Merkel cell carcinoma? *Oncogene* 2018; **37**: 1409–1416.
- Verhaegen ME, Harms PW, Van Goor JJ *et al.* Direct cellular reprogramming enables development of viral T antigen-driven Merkel cell carcinoma in mice. *J. Clin. Invest.* 2022; **132**: e152069.
- Walsh NM. Primary neuroendocrine (Merkel cell) carcinoma of the skin: morphologic diversity and implications thereof. *Hum. Pathol.* 2001; **32**: 680–689.
- Harms PW, Verhaegen ME, Hu K *et al.* Genomic evidence suggests that cutaneous neuroendocrine carcinomas can arise from squamous dysplastic precursors. *Mod. Pathol.* 2022; **35**(4):506–514.
- Kervarrec T, Appenzeller S, Samimi M *et al.* Merkel cell polyomavirus-negative-Merkel cell carcinoma originating from in situ squamous cell carcinoma: a keratinocytic tumor with neuroendocrine differentiation. *J. Invest. Dermatol.* 2022; **142** (3 Pt A):516–527.
- Martin B, Poblet E, Rios JJ *et al.* Merkel cell carcinoma with divergent differentiation: histopathological and immunohistochemical study of 15 cases with PCR analysis for Merkel cell polyomavirus. *Histopathology* 2013; **62**: 711–722.
- Kervarrec T, Aljundi M, Appenzeller S *et al.* Polyomavirus-positive Merkel cell carcinoma derived from a trichoblastoma suggests an epithelial origin of this Merkel cell carcinoma. *J. Invest. Dermatol.* 2020; **140**(5):976–985.
- Kervarrec T, Tallet A, Miquelestorena-Standley E *et al.* Diagnostic accuracy of a panel of immunohistochemical and molecular markers to distinguish Merkel cell carcinoma from other neuroendocrine carcinomas. *Mod. Pathol.* 2019; **32**(4):499–510.
- Harms KL, Healy MA, Nghiem P *et al.* Analysis of prognostic factors from 9387 Merkel cell carcinoma cases forms the basis for the new 8th edition AJCC staging system. *Ann. Surg. Oncol.* 2016; **23**: 3564–3571.
- Kervarrec T, Samimi M, Gaboriaud P *et al.* Detection of the Merkel cell polyomavirus in the neuroendocrine component of combined Merkel cell carcinoma. *Virchows Arch. Int. J. Pathol.* 2018; **472**(5):825–837.
- Jiang H, Lei R, Ding S-W, Zhu S. Skewer: a fast and accurate adapter trimmer for next-generation sequencing paired-end reads. *BMC Bioinf.* 2014; **15**: 182.

21. Martin M. Cutadapt removes adapter sequences from high-throughput sequencing reads. *EMBNET. J.* 2011; 17; 10.
22. Li H, Durbin R. Fast and accurate short read alignment with burrows-wheeler transform. *Bioinformatics* 2009; 25; 1754–1760.
23. Li H, Handsaker B, Wysoker A *et al.* The sequence alignment/map format and SAMtools. *Bioinformatics* 2009; 25; 2078–2079.
24. McKenna A, Hanna M, Banks E *et al.* The genome analysis toolkit: a MapReduce framework for analyzing next-generation DNA sequencing data. *Genome Res.* 2010; 20; 1297–1303.
25. Cibulskis K, Lawrence MS, Carter SL *et al.* Sensitive detection of somatic point mutations in impure and heterogeneous cancer samples. *Nat. Biotechnol.* 2013; 31; 213–219.
26. Wang K, Li M, Hakonarson H. ANNOVAR: functional annotation of genetic variants from high-throughput sequencing data. *Nucleic Acids Res.* 2010; 38; e164.
27. Thorvaldsdóttir H, Robinson JT, Mesirov JP. Integrative Genomics Viewer (IGV): high-performance genomics data visualization and exploration. *Brief. Bioinform.* 2013; 14; 178–192.
28. Goncarencu A, Rager SL, Li M, Sang Q-X, Rogozin IB, Panchenko AR. Exploring background mutational processes to decipher cancer genetic heterogeneity. *Nucleic Acids Res.* 2017; 45(W1); W514–W522.
29. Liang Y, Qiu K, Liao B *et al.* Seeksv: an accurate tool for somatic structural variation and virus integration detection. *Bioinformatics* 2017; 33; 184–191.
30. Collina G, Bagni A, Fano RA. Combined neuroendocrine carcinoma of the skin (Merkel cell tumor) and trichilemmal cyst. *Am. J. Dermatopathol.* 1997; 19; 545–548.
31. Ivan D, Bengana C, Lazar AJ, Diwan AH, Prieto VG. Merkel cell tumor in a trichilemmal cyst: collision or association? *Am. J. Dermatopathol.* 2007; 29; 180–183.
32. Molina-Ruiz AM, Bernárdez C, Requena L, Rütten A. Merkel cell carcinoma arising within a poroma: report of two cases. *J. Cutan. Pathol.* 2015; 42; 353–360.
33. Ogawa T, Donizy P, Wu C-L, Cornejo KM, Ryś J, Hoang MP. Morphologic diversity of Merkel cell carcinoma. *Am. J. Dermatopathol.* 2020; 42; 629–640.
34. Requena L, Jaqueti G, Rütten A, Mentzel T, Kutzner H. Merkel cell carcinoma within follicular cysts: report of two cases. *J. Cutan. Pathol.* 2008; 35; 1127–1133.
35. Su W, Kheir SM, Berberian B, Cockerell CJ. Merkel cell carcinoma in situ arising in a trichilemmal cyst: a case report and literature review. *Am. J. Dermatopathol.* 2008; 30; 458–461.
36. Sawaya JL, Khachemoune A. Poroma: a review of eccrine, apocrine, and malignant forms. *Int. J. Dermatol.* 2014; 53; 1053–1061.
37. Weber M, Nguyen MB, Li MY, Flora P, Shuda M, Ezhkova E. Merkel cell polyomavirus T-antigen-mediated reprogramming in adult Merkel cell progenitors. *J. Invest. Dermatol.* 2023; 29; S0022-202X(23)02120-6.
38. Harold A, Amako Y, Hachisuka J *et al.* Conversion of Sox2-dependent Merkel cell carcinoma to a differentiated neuron-like phenotype by T antigen inhibition. *Proc. Natl. Acad. Sci. U.S.A.* 2019; 116(40):20104–20114.
39. Zur Hausen A, Rennspies D, Winnepenninckx V, Speel E-J, Kurz AK. Early B-cell differentiation in Merkel cell carcinomas: clues to cellular ancestry. *Cancer Res.* 2013; 73; 4982–4987.
40. Borchert S, Czech-Sioli M, Neumann F *et al.* High-affinity Rb binding, p53 inhibition, subcellular localization, and transformation by wild-type or tumor-derived shortened Merkel cell polyomavirus large T antigens. *J. Virol.* 2014; 88; 3144–3160.
41. Schrama D, Sarosi E-M, Adam C *et al.* Characterization of six Merkel cell polyomavirus-positive Merkel cell carcinoma cell lines: Integration pattern suggest that large T antigen truncating events occur before or during integration. *Int. J. Cancer* 2019; 145; 1020–1032.
42. Starrett GJ, Thakuria M, Chen T *et al.* Clinical and molecular characterization of virus-positive and virus-negative Merkel cell carcinoma. *Genome Med.* 2020; 12; 30.
43. Sastre-Garau X, Peter M, Avril M-F *et al.* Merkel cell carcinoma of the skin: pathological and molecular evidence for a causative role of MCV in oncogenesis. *J. Pathol.* 2009; 218; 48–56.
44. Haugg AM, Rennspies D, zur Hausen A *et al.* Fluorescence in situ hybridization and qPCR to detect Merkel cell polyomavirus physical status and load in Merkel cell carcinomas. *Int. J. Cancer* 2014; 135; 2804–2815.
45. Fan K, Gravemeyer J, Ritter C *et al.* MCPyV large T antigen induced atonal homolog 1 (ATOH1) is a lineage-dependency oncogene in Merkel cell carcinoma. *J. Invest. Dermatol.* 2020; 140(1):56–65.e3.
46. Kervarrec T, Samimi M, Hesbacher S *et al.* Merkel cell polyomavirus T antigens induce Merkel cell-like differentiation in GLI1-expressing epithelial cells. *Cancer* 2020; 12(7):1989.
47. Kervarrec T, Chéret J, Paus R, Houben R, Schrama D. Transduction-induced overexpression of Merkel cell T antigens in human hair follicles induces formation of pathological cell clusters with Merkel cell carcinoma-like phenotype. *Exp. Dermatol.* 2022; 31(2):259–260.
48. Nemeth K, Gorog A, Mezey E *et al.* Cover image: detection of hair follicle-associated Merkel cell polyomavirus in an immunocompromised host with follicular spicules and alopecia. *Br. J. Dermatol.* 2016; 175; 1409.

Supporting Information

Additional Supporting Information may be found in the online version of this article:

Table S1. Combined tumour cases associating MCC and benign adnexal tumours component previously reported in the literature.

Table S2. Read statistics.

Table S3. Description of the somatic mutations detected by whole exome sequencing in the trichoblastoma and the MCC part of the combined tumour.

Table S4. Clinical and virologic features of VP1 expressing pure MCC cases.

Method S1. Antibodies used for Immunohistochemistry.